Available online at www.sciencedirect.com

ScienceDirect

Procedia CIRP 84 (2019) 761–768

www.elsevier.com/locate/procedia

29th CIRP Design 2019 (CIRP Design 2019)

Two extensions towards practical applications of a paradox in curved beams

Luigi Leopardi[a], Antonio Strozzi[a]*

[a]*Dipartimento di Ingegneria E. Ferrari, Università di Modena e Reggio Emilia,Via P. Vivarelli 10, Modena 41125, Italy*

* Corresponding author. Tel.: +39-059-2056147; fax: +39-059-2056126. *E-mail address:* antonio.strozzi@unimore.it

Abstract

For particular sections of a rectilinear beam subjected to bending it is possible to simultaneously lower the bending stress and reduce the beam mass, by wisely removing material from zones far from the neutral axis. It has recently been shown that an analogous paradoxical behaviour occurs in a curved beam subjected to bending, by laterally removing material from section zones close to the neutral axis. The bending stress diminution is often of the order of a few %, whereas the mass diminution may reach 10 %. To get practically more interesting results, in this paper the demanding achievement of a concurrent stress and mass reduction is relaxed in favour of two weaker requests: a) for a general section, the intrados stress is assumed as the reference stress, and the maximum mass reduction achieved by laterally removing material is sought under the condition that the intrados stress equals such reference stress; b) the intrados stress of a particular section is assumed as the reference stress, and material is laterally removed from the adjacent sections until their intrados stress equals the above reference value. Analytical applications of the two above approaches to a crane hook are carried out and compared to FE forecasts.

Peer-review under responsibility of the scientific committee of the CIRP Design Conference 2019.

Keywords: lightweight structures; design strategies; paradox of Mechanics; curved beam; optimization; stress; mass reduction; Gateaux differentiation; FE; crane hook.

1. Introduction

It is known that for particular sections of a rectilinear beam subjected to bending it is possible to simultaneously lower the bending stress and reduce the beam mass, by wisely removing material from zones far from the neutral axis, e.g. Saint Venant [1] and Timoshenko [2], see Figures 1 (a), (c), (e). It has recently been shown by Strozzi [3] that an analogous paradoxical behaviour occurs for a curved beam modelled in terms of the classical Winkler theory, e.g. Barber [4], Boresi [5]; in fact, it is sometimes possible to concurrently diminish both the intrados bending stress and the beam mass, by removing material from section zones close to the neutral axis, see Figure 1 (b) for an initially rhombic ross section, Figure 1 (d) for an initially circular section, and Figure 1 (f) for a square cross section along whose sides two rectangular grooves are machined.

For a general initial cross section of a curved beam, the zones from which a lateral material removal produces an intrados bending stress diminution have analytically been determined by Strozzi [3] through Gateaux differentiation. Such favourable zones constitute a strip, whose delimiting radii have analytically been evaluated. In the approach favoured in this study, the inner, r_i, and outer, r_o, radii of the beam

2212-8271 © 2019 The Authors. Published by Elsevier B.V.
Peer-review under responsibility of the scientific committee of the CIRP Design Conference 2019.
10.1016/j.procir.2019.04.296

cross section, Figure 1, are regarded as imposed variables, the material removal from the section sides being assumed not to modify such radii.

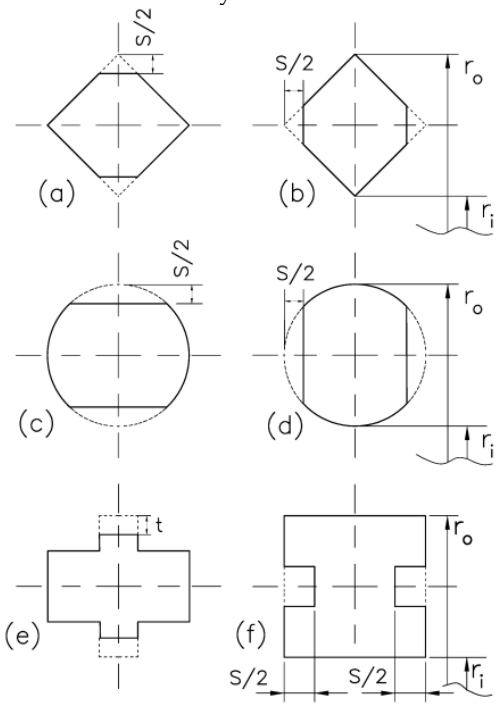

Fig. 1. (a) a rhombic section, (c) a circular section, (e) a rectangular section with projections of a rectilinear beam, in which material is removed far from the neutral axis; (b) a rhombic section, (d) a circular section, (f) a rectangular section of a curved beam, along whose sides two rectangular grooves are machined.

Unfortunately, in practical applications the bending stress diminution attainable with the paradoxical approach of Strozzi [3], is often of the order of a technically negligible 1 %, whereas the mass diminution may reach a more significant 10 %. To get practically more interesting results, in this paper the demanding achievement of a concurrent stress and mass reduction is relaxed in favour of two weaker requests; a) the intrados stress of a particular groove-free cross section is assumed as the reference stress, and the maximum mass reduction of that particular cross section, achieved by laterally removing material, is sought under the condition that the intrados stress equals such reference stress; in other words, the aim is to determine for a general section the maximum lateral mass diminution that does not modify the initial intrados stress computed for a groove-free section; b) the solution achieved defines the cross section of minimum weight that produces a desired intrados stress value. This approach is particularly useful when the section where the maximum intrados stress occurs is assumed as the beam reference section; upon lateral material removal, the stress in the adjacent understressed sections is increased until their intrados stress becomes constant, at least within a certain zone. Consequently, this approach may be of help in attaining a uniform-strength component, see the hook crane optimization presented in Section 5.

It is noted that in the first approach the beam sections are considered independently, and the most favourable groove is separately determined for all sections. In the second approach, instead, a section is assumed as the reference one, and the lateral material removal is simultaneously optimized for all beam sections falling within a certain beam region.

To further broaden the horizon of the theory developed in this paper with respect to the purely flexural approach of Strozzi [3], the simultaneous presence of bending moment and of normal force is here considered.

To derive the equations useful for optimizing the beam, a distinction is made in the selection of the parameters defining the initial and modified cross sections, see Strozzi [3]. The properties of the initial section are summarized by the section area and by its neutral and center of mass radii, whereas the section modification is described by the lateral removal of material. A Gateaux linearization is then performed to simplify the equations expressing the stress state, thus enabling explicit design formulae to be derived, and some cross section geometries to be improved.

Although this paper essentially addresses the development of some analytical models, it also provides useful practical insight into the influence on the stresses of an addition or removal of material from a cross section. Two examples convincingly evidencing the relevance of the determination of the above stress trend, extracted from the combustion engine component realm, are a) ribs projecting outwards from the outer surface of a connecting rod small end, Strozzi et al. [6], where the adoption of some rib geometries produces an unwanted stress increase; b) ribs projecting inwards from the inner surface of a hollow gudgeon pin, Strozzi et al. [7], which beneficially lower the shear stresses, but undesirably increase the bending stresses.

This paper is organized as follows. First, the paradoxical approach of Strozzi [3], producing a simultaneous stress and cross section area diminution, is briefly recalled. Secondly, the less demanding request is considered for a cross section diminution upon constancy of the intrados bending plus normal stress. In particular, the radii delimiting the widest favourable strip from which it is possible to remove material without altering the intrados stress are analytically determined with the approximate, Gateaux-linearized model. Third, the requirement for a mass diminution upon an imposed intrados stress distribution within a certain beam zone is addressed.

2. The known results

Since the method here favoured is an extension of Strozzi [3], a brief account of the known results is summarized in the following. According to the Winkler theory for curved beams, the mechanical parameters of

the beam cross section necessary for evaluating the bending and normal stresses are the section area A, the centre of mass radius r_g, the neutral radius r_n, and the radius r defining the section zone where the stresses are computed, Figure 2. In addition, r_i and r_o are the inner and outer radii, and r_1 and r_2 define a strip of material to be removed. Finally, the cumulative lateral removal depth is denoted by $s(r)$.

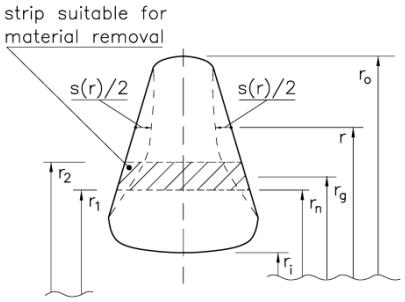

Fig. 2. Initial cross section and its modification by laterally removing material according to the cumulative removal depth function $s(r)$. Definition of the variables r_i, r_n, r_g, r, r_o, r_1, r_2, $s(r)$.

The bending, σ_M, and normal force, σ_N, stresses in a compact section of a planar, curved beam are, e.g. Barber [4] :

$$\sigma_M = \frac{M(r_n - r)}{A(r_g - r_n)r} \quad ; \quad \sigma_N = \frac{N}{A} \quad . \tag{1}$$

In the basic theory for curved beams upon which formula (1) relies, the simplifying assumption is adopted that the stress σ_N due to the normal force is uniform. To improve this approximation, correcting coefficients have been proposed, e.g. Cook [8]. For simplicity, corrective coefficients have been omitted in this paper, one of the reasons being the fact that the normal stress is generally considerably small with respect to its bending counterpart.

In Strozzi [3] it was found advantageous to make a distinction between the symbols addressing the initial and modified cross section, by summarizing the properties of the initial section through the three parameters A_0, $r_{g,0}$, $r_{n,0}$, where the index 0 denotes the initial section, and by describing the section modification through the lateral removal of material, quantified by the cumulative removal depth $s(r)$, Fig. 2.

Classical formulae, e.g. [3-5], are employed that describe the parameters of a modified section as a composition of the parameters addressing the initial section, endowed with the index 0, and of the lateral removal depth $s(r)$; the expression in terms of $s(r)$ of the purely flexural stress σ_i at the intrados radius r_i, where the maximum bending stress usually occurs, is reported in (2), (the brackets evidence the factors constituting formula (2)), where M is the bending moment, and A_0, $r_{g,0}$, $r_{n,0}$, r_i, r_o are the initial area, the radius of the centre of mass, of the neutral axis, and the inner and outer radii, respectively. In Strozzi [3] equation (2) has been simplified by linearizing the effect of the removal depth $s(r)$ through a first order Taylor expansion based upon Gateaux differentiation, see equation (3):

$$\sigma_i = \frac{M\left[\dfrac{A_0 - \int_{r_i}^{r_o} s(r)\,dr}{\dfrac{A_0}{r_{n,0}} - \int_{r_i}^{r_o} \dfrac{s(r)}{r}\,dr} - r_i\right]}{\left[A_0 - \int_{r_i}^{r_o} s(r)\,dr\right]\left[\dfrac{A_0\, r_{g,0} - \int_{r_i}^{r_o} s(r)\, r\,dr}{A_0 - \int_{r_i}^{r_o} s(r)\,dr} - \dfrac{A_0 - \int_{r_i}^{r_o} s(r)\,dr}{\dfrac{A_0}{r_{n,0}} - \int_{r_i}^{r_o} \dfrac{s(r)}{r}\,dr}\right] r_i}, \tag{2}$$

$$\sigma_i \approx \sigma_i\big|_{s=0} + G'(s=0)\,s \quad , \tag{3}$$

where G' represents the Gateaux derivative, i.e., the functional equivalent of the ordinary derivative, and it is defined as, e.g. Milne [9]:

$$G'(s=0)\,s = \lim_{\lambda \to 0} \frac{d}{d\lambda} G(\lambda s) \quad . \tag{4}$$

By Gateaux-linearizing equation 2, a remarkably simpler formula is obtained, Strozzi [3]:

$$\sigma_i \approx \frac{M(r_{n,0} - r_i)}{A_0(r_{g,0} - r_{n,0})\,r_i} - \frac{M}{A_0^2(r_{g,0} - r_{n,0})^2\,r_i} \int_{r_i}^{r_o} \frac{s(r)}{r}(r_{n,0} - r)\left[r(r_{n,0} - r_i) - r_{n,0}(r_{g,0} - r_i)\right] dr \tag{5}$$

where the first fraction of (5) expresses the initial intrados bending stress $\sigma_{i,0}$. The factor of the integrand multiplying $s(r)/r$ in (5) is null for the following two delimiting radii r_1 and r_2, Figure 2:

$$r_1 = r_{n,0} \quad ; \quad r_2 = r_{n,0}\frac{(r_{g,0} - r_i)}{(r_{n,0} - r_i)} \quad . \tag{6}$$

In addition, the above factor remains positive within the $[r_1, r_2]$ interval according to (6). Consequently, if material is removed within a strip delimited by the two radii r_1 and r_2, Figure 2, the paradoxical result is achieved according to which the intrados bending stress diminishes upon mass removal.

3. Modification of the strictly paradoxical approach by imposing the condition of unaltered intrados stress

In this Section a less stringent version is developed of the paradoxical approach, summarized in Section 2, of Strozzi [3]. It is recalled that, in the strictly paradoxical approach of Strozzi [3], a favourable strip is determined that defines the cross section zone from which it is possible to simultaneously remove material and reduce the intrados bending stress. In this Section, instead, the strip is defined that delimits the zone from which it is possible to remove the maximum amount of material without altering the intrados stress occurring in a laterally groove-free section. To achieve more general results with respect to the purely flexural model of Strozzi [3], the stress due to the concurrent presence of both the bending moment and the normal force is accounted for in this Section.

By considering equations (1) and (2), the sum, σ_i, of the intrados bending and normal stresses provides equation (7). The Gateaux linearization of equation (7) provides equation (8):

$$\sigma_i = \frac{M\left[\dfrac{A_0-\int_{r_i}^{r_o} s(r)\,dr}{\dfrac{A_0}{r_{n,0}}-\int_{r_i}^{r_o}\dfrac{s(r)}{r}\,dr}-r_i\right]}{\left[A_0-\int_{r_i}^{r_o} s(r)\,dr\right]\left[\dfrac{A_0\,r_{g,0}-\int_{r_i}^{r_o} s(r)\,r\,dr}{A_0-\int_{r_i}^{r_o} s(r)\,dr}-\dfrac{A_0-\int_{r_i}^{r_o} s(r)\,dr}{\dfrac{A_0}{r_{n,0}}-\int_{r_i}^{r_o}\dfrac{s(r)}{r}\,dr}\right]r_i}+\frac{N}{A_0-\int_{r_i}^{r_o} s(r)\,dr}. \quad (7)$$

$$\sigma_i \approx \frac{M\left(r_{n,0}-r_i\right)}{A_0\left(r_{g,0}-r_{n,0}\right)r_i}+\frac{N}{A_0}- \quad (8)$$

$$\frac{M}{A_0^2\left(r_{g,0}-r_{n,0}\right)^2 r_i}\int_{r_i}^{r_o}\frac{s(r)}{r}\left(r_{n,0}-r\right)\left[r\left(r_{n,0}-r_i\right)-r_{n,0}\left(r_{g,0}-r_i\right)\right]dr+\frac{N}{A_0^2}\int_{r_i}^{r_o} s(r)\,dr.$$

A positive value of M produces a positive intrados bending stress; a positive N causes a tensile stress; a positive value of $s(r)$ describes a lateral removal of material, Figure 2, that is, it defines the profile of a lateral lightening cavity; $s(r)$ is non null only within the interval delimited by the radii r_1 and r_2 defining the lightening pocket width, and it is null elsewhere.

It is technically suitable to adopt a lightening pocket of rectangular profile, described by a constant value for s within the interval defined by the radii r_1 and r_2, and by a null value elsewhere. However, a rectangular lightening pocket produces an undesired logarithmic term in equation (8), that precludes the possibility of deriving closed form analytical expressions for the radii r_1 and r_2 delimiting the lightening pocket. To avoid such term, a physically sound simplifying assumption consists in describing $s(r)$ as linearly proportional to r according to the expression:

$$s(r)=\frac{2\,S\,r}{r_1+r_2} \quad , \quad (9)$$

where S is a constant quantifying the mean, cumulative, groove depth, Figure 1 (f). The depth of the pocket bottom described by this approximation is therefore not constant, but it varies linearly with r. This pocket shape is an approximation of a technically more realistic pocket with constantly deep bottom. Comments on the validity of this approximation are supplied in Sections 3 and 4. The two auxiliary integrals I_M and I_N are then introduced:

$$I_M=\int_{r_1}^{r_2}\frac{s(r)}{r}\left(r_{n,0}-r\right)\left[r\left(r_{n,0}-r_i\right)-r_{n,0}\left(r_{g,0}-r_i\right)\right]dr=$$
$$-\frac{S}{3\left(r_1+r_2\right)}\left[2\left(r_{n,0}-r_i\right)\left(r_2^3-r_1^3\right)-3r_{n,0}\left(r_{n,0}+r_{g,0}-2r_i\right)\left(r_2^2-r_1^2\right)+6r_{n,0}^2\left(r_{g,0}-r_i\right)\left(r_2-r_1\right)\right] \quad (10)$$
$$I_N=\int_{r_{k,1}}^{r_{k,2}} s(r)\,dr=S\left(r_2-r_1\right) \quad ,$$

where the right-hand sides of (10) have been obtained by introducing expression (9) for $s(r)$ into I_M and I_N. The sum of the bending and normal stresses at the intrados is expressed in (11) in terms of the two integrals I_M and I_N as:

$$\sigma_i \approx \frac{M\left(r_{n,0}-r_i\right)}{A_0\left(r_{g,0}-r_{n,0}\right)r_i}+\frac{N}{A_0}-\frac{M}{A_0^2\left(r_{g,0}-r_{n,0}\right)^2 r_i}I_M+\frac{N}{A_0^2}I_N \quad . \quad (11)$$

The condition of unaltered intrados stress σ_i in a grooved section with respect to a groove-free cross section thus becomes:

$$M\,I_M-N\,I_N\left(r_{g,0}-r_{n,0}\right)^2 r_i=0 \quad , \quad (12)$$

or, alternatively, by employing the extended expressions for I_M and I_N:

$$2M\left(r_{n,0}-r_i\right)\left(r_1^2+r_1\,r_2+r_2^2\right)+3\left(r_1+r_2\right)\left[N\,r_i\left(r_{g,0}-r_{n,0}\right)^2-M\,r_{n,0}\left(r_{n,0}+r_{g,0}-2r_i\right)\right]+$$
$$6Mr_{n,0}^2\left(r_{g,0}-r_i\right)=0 \quad . \quad (13)$$

To achieve the maximum mass diminution under the condition of unvaried intrados stress, i.e., to define the most favourable strip, equation (13) must be coupled to an additional equation expressing that the favourable strip width be maximum. Consequently, the condition is added that imposes the stationarity condition $\mathrm{d}(r_2-r_1)/\mathrm{d}r_1=0$ evaluated through implicit differentiation:

$$M\left(r_{n,0}-r_i\right)\left(r_1+r_2\right)+N\,r_i\left(r_{g,0}-r_{n,0}\right)^2-M\,r_{n,0}\left(r_{g,0}+r_{n,0}-2r_i\right)=0 \quad . \quad (14)$$

The physically acceptable analytical solution in terms of r_1 and r_2 of the system of the two nonlinear equations (13) and (14) is:

$$r_1\left[2\left(r_{n,0}-r_i\right)M\right]=-\sqrt{3}\left(r_{g,0}-r_{n,0}\right)\sqrt{r_i^2\left(r_{g,0}-r_{n,0}\right)^2N^2-2r_i\,r_{n,0}\left(r_{g,0}+r_{n,0}-2r_i\right)MN+r_{n,0}^2M^2}-$$
$$r_i\left(r_{g,0}-r_{n,0}\right)^2N+r_{n,0}\left(r_{g,0}+r_{n,0}-2r_i\right)M$$
$$r_2\left[2\left(r_{n,0}-r_i\right)M\right]=\sqrt{3}\left(r_{g,0}-r_{n,0}\right)\sqrt{r_i^2\left(r_{g,0}-r_{n,0}\right)^2N^2-2r_i\,r_{n,0}\left(r_{g,0}+r_{n,0}-2r_i\right)MN+r_{n,0}^2M^2}-$$
$$r_i\left(r_{g,0}-r_{n,0}\right)^2N+r_{n,0}\left(r_{g,0}+r_{n,0}-2r_i\right)M \quad . \quad (15)$$

The achievement of the closed form analytical expressions (15) for r_1 and r_2 has been made possible by the simplifications accomplished with Gateaux linearization. The achievement of similar formulae based upon the exact expression (7) for the intrados stresses would be prohibitively complex.

3.1. Numerical example: square section endowed with lateral rectangular grooves that do not alter the intrados stress

To get some indications about the attainable mass reduction without modifying the intrados stress, a curved beam is examined, whose square section is endowed with lateral rectangular grooves that preserve the intrados stress.

In Figure 3 of Strozzi [3] the intrados stress diminution was evaluated for an initially square cross section, along whose sides two lateral rectangular grooves had been manufactured. In Figure 3 of this paper the parallel problem of the achievable mass diminution upon the condition of unaltered (and not reduced) intrados stress is considered. For simplicity, a purely flexural loading has been assumed. The following values of the variables have been adopted: r_i=1, r_o=2, b=1. The two roots defining the favourable strip in this intrados iso-stress condition, computed with formulae (15), are r_1=1.374 and r_2=1.698.

The curve of Figure 3 reports the intrados bending stress increase $\Delta\sigma_i$ normalized over the initial intrados stress $\sigma_{0,i}$, as a function of the normalized cumulative groove depth S/b, for a rectangular groove whose delimiting radii have been computed from formulae (15).

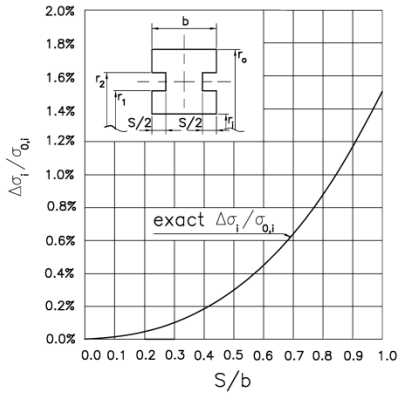

Fig. 3. Normalized intrados bending stress increase $\Delta\sigma_I/\sigma_{0,i}$ in terms of normalized cumulative groove depth S/b.

This stress variation is null when computed with the Gateaux linearized formula (8). In fact, it is recalled that expressions (15) of the radii delimiting the favourable strip have been derived by imposing that the intrados bending stress remains unaltered according to the Gateaux approximate model. This null curve has been omitted in Figure 3. Instead, the relative stress variation evaluated according to the exact theory of formula (7) deviates from 0, albeit moderately, and it has been reported in Figure 3 to provide information on the error incurred in the Gateaux linearization. In the exact theory the groove bottom is assumed of constant depth, whereas in the Gateaux modelling the bottom varies with r according to (9). From equation (9) the groove bottom depth measured for $r=r_2$ is 10 % higher than its counterpart for $r=(r_1+r_2)/2$.

The marginal increase perceivable in Figure 3 of a few per cent of the intrados bending stress obtained by employing the exact model (7) and a rectangular groove with constant bottom depth, where the delimiting radii of equations (15) have been computed from the Gateaux linearized approach, suggests that the cumulative error incurred in the Gateaux linearization (8) and in the approximate description (9) of a rectangular groove be limited.

The mass diminution of Figure 3 is appreciably higher than that referring to the paradoxical approach of Strozzi [3]. In fact, by imposing S/b=0.5 (an excessively thin hub thickness is technically unacceptable), the area reduction is (1.698-1.374)×0.5=0.1620, which implies a section diminution of 16 %. Moving to the purely paradoxical approach of Strozzi [3], the area diminution is (1.629-1.442)×0.5=0.0935, with a lower section diminution of 9.3 %. This example shows that the approach favoured in this paper, relaxing the request for concurrent area and stress diminution of Strozzi [3] in favour of a weaker condition of unvaried intrados bending stress, allows an appreciably higher cross section diminution; for this geometry of the beam cross section, the mass diminution is 1.7 times that achieved in the paradoxical condition.

4. Modification of the strictly paradoxical approach to attain a required distribution of the intrados stress

An alternative approach to Section 3 for reducing weight is to require that the radial extent of the lightening pocket produces a constant intrados stress with respect to a reference value when considering various sections along the beam axis. With this approach an optimized uniform-strength shape may be achieved.

In the following the radii delimiting the lateral pockets are evaluated for an imposed intrados stress. From the linearized equation (11) the condition that the intrados bending plus normal stress equals the imposed value σ_I may be formulated as:

$$\sigma_i A_0 = \frac{M}{\left(r_{g,0}-r_{n,0}\right) r_i}\left[r_{n,0}-r_i-\frac{I_M}{A_0\left(r_{g,0}-r_{n,0}\right)}\right]+N\left[1+\frac{I_N}{A_0}\right] \quad . \tag{16}$$

By introducing into (16) expressions (10) for the integrals I_M and I_N, one obtains:

$$\sigma_i A_0 = \frac{M}{3\,r_i A_0\left(r_{g,0}-r_{n,0}\right)^2\left(r_1+r_2\right)}\times \tag{17}$$
$$\left\{S\left[2\left(r_{n,0}-r_i\right)\left(r_2^3-r_1^3\right)-3r_{n,0}\left(r_{n,0}+r_{g,0}-2r_i\right)\left(r_2^2-r_1^2\right)+6r_{n,0}^2\left(r_{g,0}-r_i\right)\left(r_2-r_1\right)\right]+\right.$$
$$\left.3\left(r_1+r_2\right)\left(r_{g,0}-r_{n,0}\right)\left(r_{n,0}-r_i\right)A_0\right\}+N\left[1+\frac{S\left(r_2-r_1\right)}{A_0}\right] \quad .$$

Similar to Section 3, the second equation necessary for evaluating r_1 and r_2 stems from the requirement of the stationarity condition $\mathrm{d}(r_2-r_1)/\mathrm{d}r_1=0$ evaluated through implicit differentiation. The corresponding equation is:

$$\left(r_1^2+r_2^2+4r_1r_2\right)\left(r_{n,0}-r_i\right)-6\left(r_{g,0}-r_i\right)r_{n,0}^2=0 \quad . \tag{18}$$

An analytical solution to the system formed by the nonlinear equations (17) and (18) in terms of the radii r_1 and r_2 delimiting the groove has been achieved, but it is too long to be reported here.

4.1. Numerical example: imposition of an intrados stress value in a square section endowed with lateral rectangular grooves

The following example evidences the possibility of forecasting the cross section modifications that produce a prescribed value of the intrados stress. More precisely, the approach here developed optimizes the radii delimiting the most favourable zone from which to remove material. The geometry considered is similar to that of Figure 3; it is a square section endowed with two lateral grooves, Figure 4. For simplicity, a purely flexural loading has been assumed. The following values of the variables have been adopted: r_i=1, r_o=2, b=1, $S=b/2$. The x-axis reports $\sigma_i/\sigma_i|_{S=0}$, where σ_i denotes the imposed value of the intrados stress, and $\sigma_i|_{S=0}$ is a reference variable, expressing the intrados stress in the absence of lateral grooves. The left y-axis reports the two radii r_1 and r_2, computed from expressions (17) and (18) deriving from Gateaux linearization, defining the width of the rectangular

groove that produces the imposed value of the intrados stress σ_i. (The cumulative groove depth is expressed by S, and its value is kept fixed in this example.)

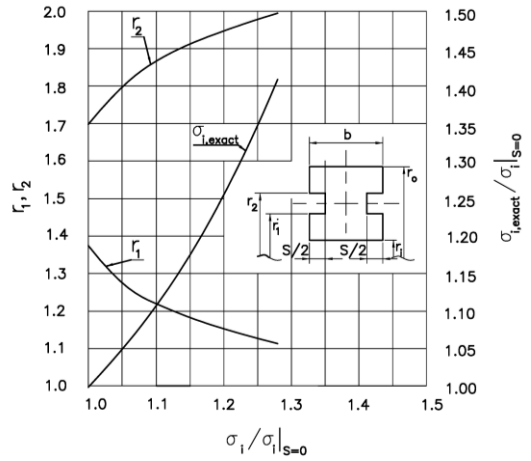

Fig. 4. radii r_1 and r_2 delimiting the groove in terms of imposed intrados stress σ_i; exact stress versus Gateaux linearized stress.

The right y-axis reports the normalized exact intrados stress $\sigma_{i,exact}$, computed from the exact expression (7) (and not from the Gateaux linearized expression (8)), with reference to a groove shape defined by the above values of r_1 and r_2, and by the imposed value of S.

If the Gateaux linearization provided exact results, the curve reporting the normalized $\sigma_{i,exact}$ value would be linear, and it would mirror the x values over the y-axis. Instead, Figure 4 shows that the above curve is moderately superlinear, thus indicating that the nonlinear effects are limited in this example; in addition, the above curve does not exactly pass through the origin of the diagram, since the Gateaux calculations have been developed for a moderately inclined groove bottom according to expression (9), whereas in the exact calculations the groove was of constant depth. The smallness of the above offset confirms that the effect of the slope of the groove bottom is limited.

For a unity x-variable, that is, for an imposed value of σ_i equal to that occurring in the absence of lateral grooves, the radii delimiting the groove whose presence does not modify the intrados stress, Section 3, are r_1=1.374 and r_2=1.698. When the imposed intrados stress is increased, the equivalent for curved beams of the section modulus in rectilinear beams must decrease and, therefore, the groove width , i.e. r_2-r_1, must increase, as it appears from Figure 4. For x=1.2, that is, for an intrados stress 1.2 times that computed in the absence of groove, and for a fixed bending moment, the two radii delimiting the groove are r_1=1.151 and r_2=1.949, thus evidencing a noticeable increase of r_2-r_1,. The corresponding section diminution is (1.949-1.151)×(1/2)=0.399, that is, it is about 40 % of the unity section without grooves.

For an x-value in the region of 1.3, the radius r_2 defining the groove upper border reaches the section outer border r_o. When the wings of an I shaped section become too thin, additional stresses occur as a result of the wing bending, [4,5], and the Winkler theory should be corrected accordingly. This correction is beyond the scope of this paper.

This example clarifies that the theory developed in this paper helps in predicting which groove dimensions produce a prescribed intrados stress. With this theory it is therefore possible to lighten the beam portions that are understressed with respect to the stress occurring in a reference section. Material may thus be removed from the undestressed regions, until their intrados stress equals the reference threshold, thus achieving a uniform-strength beam. An example of such optimization is presented in the following Section.

5. Optimization of a crane hook with initially square cross section

According to the pertinent literature, a crane hook may be optimized by a) modifying a reference trapezoidal shape, upon the imposition that the intrados and estrados stresses be equal, e.g. Dragoni [10]; b) increasing the outer radius in the zones where the maximum bending moment occurs, to limit the stresses, e.g. Strozzi et al. [6], [11]; c) machining lateral grooves, which, if wisely shaped, may lower the hook weight without significantly increasing the stresses, e.g. Strozzi [3], Jani et al. [12]. A peculiar merit of the third approach is that the caliper of the initial section is not increased by the optimization process achieved by machining lateral grooves. Only this third approach is addressed here.

Following Ratnakumar et al. [13], a crane hook of square cross section is considered. The radius of curvature has been assumed of 30 mm, and the length of the sides of the square section is 12 mm; the applied load P is 5600 N. Consequently, the inner radius r_i=24 mm, the outer radius r_o=36 mm, the centre of mass radius $r_{g,0}$=30 mm, the neutral radius $r_{n,0}$=29.5956 mm, the cross section A_0=144 mm^2. The cumulative groove depth S has been imposed to be constantly 4.8 mm.

For a general hook section defined by the angle θ shown in Figure 5 (a), the bending moment M is $P\, r_{g,0} \sin\theta$=168 $\sin\theta$ [Nm], whereas the normal force N is $P \sin\theta$=5600 $\sin\theta$ [N]. Consequently, the maximum bending moment M is 168 Nm, and the corresponding normal force N is 5600 N. The analytical maximum intrados bending stress is $M(r_{n,0}-r_i)/[A_0(r_{g,0}-r_{n,0})r_i]$=672.70 MPa; the maximum normal stress is 38.89 MPa; the maximum total intrados stress is 711.59 MPa.

Figure 5 (b) reports the FE von Mises equivalent stress for the initial square section, i.e., in the absence of lateral grooves. The commercial FE salome_meca code_aster open_source version 2018 has been employed. Details on the mesh adopted and on its suitability are omitted for brevity. The hook has been clamped along the upper sections of Figures 5 (b-d), and

loaded in *B* of Figure 5 (a) by a vertical, highly concentrated, linear force *P*, modelled with a uniformly distributed pressure acting along three adjacent rows of intrados nodes.

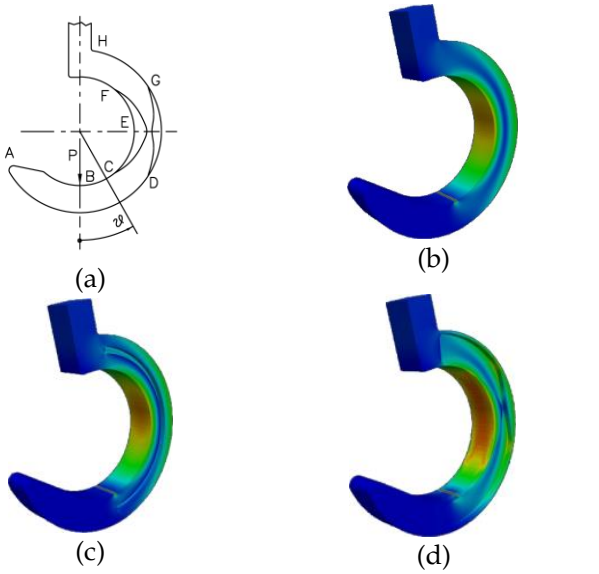

Fig. 5. (a) initial geometry; (b) von Mises stress field for initial geometry; (c) stress field for the iso-stress condition of Section 3; (d) stress field for the uniform strength condition of Section 4.

For the initial geometry, the maximum stress occurs at the intrados for $\theta=\pi/2$. Two optimizations are considered: a) the determination of the radii delimiting the two lateral grooves of the rectangular cross section, as in Figure 3, so that for a general section the intrados stress equals its ungrooved analogue, see Section 3; b) the determination of the radii delimiting the two lateral grooves of the rectangular cross section so that the intrados stress computed for a general section equals the stress value evaluated for a reference section, here assumed as the section where the intrados stress is maximum, i.e. $\theta=\pi/2$, see Section 4. With this approach, a partly uniform-strength hook is achieved.

The first kind of optimization is considered in the following. Figure 5 (c) addresses a hook along whose lateral faces a rectangular groove is manufactured following the theory of Section 3 and the previous approach a). Since for the hook loading the bending moment *M* is proportional to the normal force *N* for any θ value, the radii delimiting the groove width remain constant with θ; their values r_i=29.52 mm, r_o=31.78 mm, computed with formulae (15) of Section 3, ensure that, for a general hook section, the initial stress in the absence of grooves is not modified by the groove machining. The angular extent of the hook grooved portion is delimited by the points *B* and *H* of Figure 5 (a). Comparison between the FE forecasts of Figures 5 (b) and (c) shows that for a general section the intrados stress of Figure (c), computed in the presence of the groove, remains similar to that of Figure (b), computed in the absence of the groove. The error is evaluated by comparing analytical and FE forecasts. The FE intrados stress for $\theta=\pi/2$ of the ungrooved hook of Figure (b) is 631.0 MPa, whereas its grooved counterpart is 691.0 MPa, the relative variation being 9 %. The analytical Winkler maximum intrados stress for the grooved geometry is 711.59 MPa, and its deviation from its FE analogue is 2.9 %. The good agreement between analytical and FE predictions confirms the validity of the analytical optimization approach of Section 3.

For the technically reasonable value of the cumulative groove depth *S* of 4.8 mm, the volume of the grooved portion delimited by the points *B* and *H* of Figure 5 (a) is 11580.88 mm^3, whereas its ungrooved counterpart is 12549.57 mm^3, the volume reduction with respect to the ungrooved geometry being 7.72 %.

The second kind of optimization is considered in the following. According to the theory of Section 4 and to the previous point b), in Figure 5 (d) a lateral groove is machined that increases the intrados stresses in the initially understressed regions. The reference intrados stress is the bending plus normal stress for $\theta=\pi/2$, i.e. at the intrados point *E* of Figure 5 (a). For the sections adjacent to $\theta=\pi/2$ the adoption of an increasingly wide groove rises the intrados stress up to the reference stress of Figure (b) at point *E* of Figure (a) . This increase in the groove width favorably reduces the hook mass.

The values adopted for the radii delimiting the groove width have been numerically computed by solving the system of equations (16) and (17) of Section 4; their profile is represented in Figure 5 (a). At the point *E*, the groove delimiting radii coincide with those of Figure 5 (c), whereas for the remaining, initially understressed, hook sections, the groove width increases in order to get an iso-stress zone.

Moving along the inner (outer) radius, two angular positions defined by the letters *C* and *F* (*D* and *G*) exists for which the internal (external) groove delimiting radius reaches the hook inner (outer) radius, so that this theory is no longer rigorously applicable beyond the previous angular extents. An initially rectangular hook section with longer sides in the radial direction is expected to permit a higher hook angular portion to be optimized. The influence of the hook section shape on the hook optimization potentials is beyond the scope of this paper.

To assess practically the theory here favoured, it was decided to endow the hook inner (outer) border external to the arcs defined by the points *C* and *F* (*D* and *G*) with a thin wing smoothly varying between 0.5 and 1 mm, see the FE study of Figure 5 (d). This wing thickness has not been optimized.

Comparison between the FE forecasts of Figures (b) and (d) evidences that the *C F* angular portion exhibits an essentially constant intrados stress, equal to the grooveless stress of Figure (b) computed for $\theta=\pi/2$. This means that the hook exhibits a reasonably uniform strength within the above angular extent. In particular, the FE intrados stress for $\theta=\pi/2$ of the ungrooved hook

of Figure (b) is 631.0 MPa, whereas its grooved counterpart is 711.0 MPa, the relative error being 12 %.

The intrados stresses along the two transitional angular intervals defined by the points *C, D* and *F, G* (the angle vertex falls at the hook centre, Figure 5 (a)), smoothly deviate from constancy; in fact, it has already been noted that within such transitional angular intervals the theory of Section 4 is not rigorously applicable, since the outer border outside the arc *D G* has been endowed with wings that are extraneous to the approach of Section 4.

For *S*=4.8 mm, and limiting ourselves to the hook grooved angular portion between *D* and *G*, where the theory favoured in this paper is fully applicable, the volume of the grooved portion angularly defined by the points *D* and *G* is 5166.43 mm^3, whereas its ungrooved analogue was 6787.42 mm^3, the volume reduction with respect to the ungrooved geometry being a technically interesting 23.88 %. For comparison, in Ratnakumar et al. [13] an essentially numerical hook optimization produced a hook weight reduction of 18 % coupled to a stress increase of 6.79 %, see their Conclusions.

Table 1 collects relevant analytical and FE stresses.

	stress [MPa] for $\theta=\pi/2$			
	first optimization		second optimization	
	ungrooved	grooved	ungrooved	grooved
analytical	711.59	711.59	711.59	711.59
FE	631.00	691.00	631.00	711.00

Table 1: intrados analytical and FE stresses for $\theta=\pi/2$, for the first (see Section 3) and second (see Section 4) optimization, and for grooved and ungrooved geometries.

This example evidences the possibility of optimizing a hook analytically, FEs providing a subsidiary check.

6. Conclusions

It has recently been shown that a paradoxical behaviour occurs in a curved beam subjected to bending and modelled in terms of the classical Winkler theory, according to which it is possible to reduce the intrados stress by removing material from section zones close to the neutral axis. The bending stress diminution attainable with this paradoxical approach is often of the order of a technically negligible 1 %, whereas the mass diminution may reach a more significant 10 %. To get practically more interesting results, in this paper the demanding achievement of a concurrent stress and mass reduction has been relaxed in favour of two weaker requests; a) for a particular cross section the intrados stress has been assumed as the reference stress, and the maximum mass reduction of that particular section, achieved by laterally removing material, has been sought under the condition that the intrados stress equals such reference stress; in other words, for a general cross section the maximum mass reduction has been sought that does not alter the initial intrados stress; b) the intrados stress of a particular section has been assumed as the reference stress, and material is laterally removed from the adjacent sections until their intrados stress equals the above reference value; in other words, a beam of constant intrados stress (within a certain zone), i.e., a uniform strength beam, has been achieved. An analytical application to a crane hook has been developed, showing that a mass reduction up to about 24 % may be achieved without significantly altering the intrados bending stress. Selected comparisons with FE forecasts essentially confirm the validity of the analytical optimization approach favoured in this paper.

References

[1] Navier, CLMH. *De la résistance des corps solides. 3 ed. avec des notes et des appendices par M. Barre de Saint–Venant*. Paris: Dunod, 1864, pp. 95-99.

[2] Timoshenko, S. *Strength of Materials.* New York: John Willey and Sons, 1930, pp. 98-101.

[3] Strozzi, A., Bertocchi, E., Mantovani, S., 2018. A paradox in curved beams. Preprint *Proc. IMechE Part C: J Mech. Engng Sci*, doi:10.1177/0954406218797980.

[4] Barber, J.R. *Intermediate Mechanics of Materials* (Vol. 175). Springer Science & Business Media, 2010, p. 491.

[5] Boresi, A.P., Schmidt, R.J., Sidebottom, O.M., 1993. *Advanced Mechanics of Materials*, Wiley, N.Y., p. 368.

[6] Strozzi, A., Baldini, A., Giacopini, M., Bertocchi, E., Mantovani, S., 2016. A repertoire of failures in connecting rods for internal combustion engines, and indications on traditional and advanced design methods. *Engng Failure Analysis* , 60, pp. 20-39.

[7] Strozzi, A., Baldini, A., Giacopini, M., Bertocchi, E., Mantovani, S., 2018. A repertoire of failures in gudgeon pins for internal combustion engines. *Engng Failure Analysis* , 87, pp. 22-48.

[8] Cook R.D. Circumferential stresses in curved beams, 1992. *Trans. ASME, J Appl Mech*; 59, pp. 224–225; see also Discussion, pp. 1044-1045.

[9] Milne R.D. *Applied Functional Analysis: an Introductory Treatment*. Pitman Publishing, 1980, p. 289.

[10] Dragoni E., 2001. Designing the cross-section of curved beams for equal magnitude of peak bending stresses. *J. Strain Anal Eng Des* , 36(5), pp. 473-479.

[11] Strozzi, A. *Foundations of Machine Design.* Bologna, Italy; Pitagora, 2016 (In Italian).

[12] Jani, T.P., Biholarav, P.G., Solanki, N.R., Jivani, D.J., Rathour, M.A.N., Darji, P.H., 2015. Weight optimization of crane hook having 8 tons load capacity by modifying cross section. *Int. J. of Innovative Research in Advanced Eng*, 2(4), pp. 160-163.

[13] Ratnakumar, G.E.V., Kumar, B.J., Prasad, K., 2014. Design and stress analysis of various cross section of hook. *International Journal of Innoations in Engineering and Technology* (IJIET), pp. 90-97.